Specific absorption rate and temperature distributions in human head subjected to mobile phone radiation at different frequencies

Teerapot Wessapan [a], Siramate Srisawatdhisukul [b], Phadungsak Rattanadecho [b,*]

[a] Department of Mechanical Engineering, Faculty of Engineering, Eastern Asia University, Pathumthani 12110, Thailand
[b] Research Center of Microwave Utilization in Engineering (R.C.M.E.), Department of Mechanical Engineering, Faculty of Engineering, Thammasat University (Rangsit Campus), Pathumthani 12120, Thailand

ARTICLE INFO

ABSTRACT

This study presents a numerical analysis of specific absorption rate (SAR) and temperature distributions in the realistic human head model exposed to mobile phone radiation at 900 MHz and 1800 MHz. In the realistic human head model, the effects of operating frequency and gap distance between the mobile phone and the human head on distributions of specific absorption rate and temperature profile within the human head are systematically investigated. This study focuses attention on each tissue in the human head in order to investigate the effects of mobile phone radiation on the human head. The SAR and the temperature distribution in various tissues in human head during exposed to mobile phone radiation, obtained by numerical solution of electromagnetic wave propagation and unsteady bioheat transfer equations, are presented. For both frequencies, the highest SAR values are obtained in the region of the skin near the antenna. It is found that the highest SAR values are 0.823 W/kg and 1.187 W/kg for the frequencies of 900 MHz and 1800 MHz, respectively. The SAR values obtained from this study are well below ICNIRP limit for all cases. In addition, it is found that the temperature distributions are not directly proportional to the local SAR values. Moreover, the experimental validation has been carried out by using the infrared camera in order to complement the simulation results.

© 2011 Elsevier Ltd. All rights reserved.

1. Introduction

In recent years, there is an increasing public concern about the health implications of the use of mobile phone, as a result of the rapid growth in the use of mobile phone throughout the world. Although the safety standards are regulated in terms of the peak specific absorption rate (SAR) value of tissue, the maximum temperature increase in the human head caused by electromagnetic energy absorption is an actual influence of the dominant factors which induce adverse physiological effects. The severity of the physiological effect produced by small temperature increases can be expected to worsen in sensitive organs. Actually, a small temperature increase in the brain about 3.5 °C is noted to be an allowable limit which does not lead to physiological damage [1]. Additionally, it is reported that a very small temperature increase in hypothalamus of 0.2–0.3 °C leads to altered thermoregulatory behavior [2]. There have been reports on the effects of mobile phone radiation on the human head. The analysis generally has been conducted based on peak SAR which follows public safety standards regulation [3,4]. Due to ethical consideration, exposing a human to electromagnetic fields for experimental purposes is

limited. It is more convenient to develop a realistic human head model through numerical simulation. Numerical analysis of human head exposed to mobile phone radiation has provided useful information on absorption of electromagnetic energy for the human head under a variety of exposure condition.

Recently, the modeling of electromagnetic induced heat transport in human tissues has been investigated [5–11]. Thermal modeling of human tissue is important as a tool to investigate the effect of external heat sources as well as in predicting the abnormalities within the tissue. Most studies of heat transfer analysis in biological tissue have frequently used bioheat equation. Pennes's bioheat equation, introduced by Pennes [5] based on the heat diffusion equation, is a frequently used for analysis of heat transfer in biological tissues. The studies of high temperatures tissue ablation using a modified bioheat equation to include tissue internal water evaporation during heating have been proposed by Yang et al. [6]. The simulation result is found in agreement with experimental results. Okajima et al. [7] derived the dimensionless steady-state solutions of bioheat transfer equation to discuss the bioheat transfer characteristics common to all organs or tissues. Chua and Chou [8] have developed a bioheat model to study the freeze–thaw thermal process of cryosurgery. Recently, porous media models have been utilized to study the bioheat transport in biological media [9,10]. Many studies have been conducted using the coupled model

* Corresponding author. Tel.: +66 0 2564 3001 9; fax: 66 0 2564 3010.
  E-mail address: ratphadu@engr.tu.ac.th (P. Rattanadecho).

Nomenclatures

C	specific heat capacity (J/(kg K))	σ	electric conductivity (S/m)
E	electric field intensity (V/m)	ω	angular frequency (rad/s)
f	frequency of incident wave (Hz)	ρ	density (kg/m^3)
j	current density	ω_b	blood perfusion rate (1/s)
k	thermal conductivity (W/(m K))		
n	refractive index	*Subscripts*	
Q	heat source (W/m^3)	b	blood
T	temperature (K)	*ext*	external
t	time	*met*	metabolic
		r	relative
Greek letters		0	free space
μ	magnetic permeability (H/m)		
ε	permittivity (F/m)		

of bioheat equation and Maxwell's equation [13–15]. In the past, the experimental data on the correlation of SAR levels to the temperature increases in human head is sparse. Most previous studies of human exposed to electromagnetic field did not consider heat transfer cause an incomplete analysis to result. Therefore, modeling of heat transport in human tissues is needed to be cooperated with electromagnetic in order to completely explain the actual behavior of the transport phenomena within the human head. The topic of temperature increase in human tissue caused by exposure to electromagnetic wave, particularly those radiated by mobile phone, has been of interest for several years [12].

However, most studies of electromagnetic wave exposure of human head have not been considering realistic domain with complicated organs of several types of tissue, and experimental validation is limited or non-existent. There are few studies on the thermal field and electromagnetic field interaction in realistic physical model of the human head due to the complexity of the problem, even though it is directly related to the thermal injury of tissues. Moreover, in general situations involving near-field exposures, it is well known that the exposure conditions such as operating frequency and the gap distance between electromagnetic source and exposed object play an important role in electromagnetic energy absorption. Therefore, in order to provide information on levels of exposure and health effects from mobile phone radiation adequately, it is essential to simulate both of electromagnetic field and heat transfer within an anatomically based human head model under various exposure conditions.

Recently, our research group has tried to investigate the temperature increase in the human tissues subjected to electromagnetic wave numerically. Wessapan et al. [13,14] utilized a 2D finite element model to obtain the SAR and temperature increase in human body exposed to electromagnetic wave with different testing condition. They developed a set of governing equations utilizing the bioheat equation coupled with the Maxwell equation. The results of this study show that the dielectric and thermal properties of the tissues are play the significant role on heat transfer in human body. Keangin et al. [15] carried out on the numerical simulation of liver cancer treated by using microwave coaxial antenna. Their results are found to be in good agreement with those from the previous experimental and numerical studies under various treatment conditions.

This research is a pioneer work that simulates the SAR distribution and temperature distribution through an anatomically based human head under electromagnetic radiation. In this study, a three-dimensional realistic human head model was used to simulate the SAR distribution and temperature distribution over the realistic human head at different frequencies and gap distances. Electromagnetic wave propagation in human head was calculated using Maxwell's equations. An analysis of heat transfer in human

head exposed to electromagnetic wave was calculated using the bioheat equation. The effects of operating frequencies (900 MHz and 1800 MHz) and gap distances between the mobile phone and the human head (0 cm, 1.0 cm and 2.0 cm) on distributions of SAR and temperature distributions within the human head are systematically investigated. The frequencies of 900 MHz and 1800 MHz were chosen for simulations in this study, as they have wavelengths in the microwave band and are used frequently in area of mobile phone usage. In order to complement the simulation results, the experimental validation have been carried out by using the infrared camera. The obtained values provide an indication of limitations that must be considered for temperature increases due to electromagnetic energy absorption from mobile phones.

2. Formulation of the problem

Fig. 1 shows the radiation of electromagnetic energy from mobile phone to a realistic human head model. Due to ethical consideration, exposing a human to electromagnetic fields for experimental purposes is limited. It is more convenient to develop a realistic human head model through numerical simulation. The next section, an analysis of specific absorption rate and heat transfer in the layered human head exposed to mobile phone radiation is illustrated. The system of governing equations as well as initial and boundary conditions are solved numerically using the finite element method (FEM) via COMSOL^{TM} Multiphysics.

3. Methods and model

The first step in evaluating the effects of a certain exposure to radiation in the human head is the determination of the induced
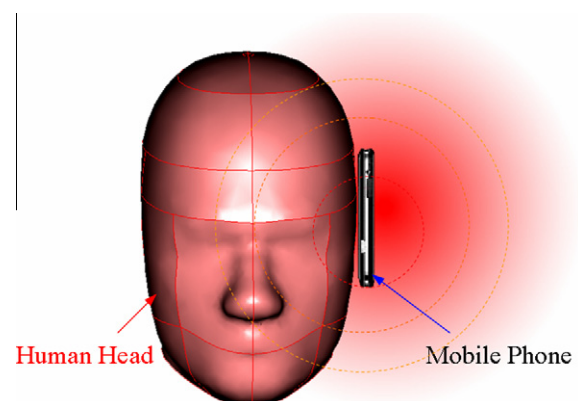

Fig. 1. Human head exposed to mobile phone radiation.

internal electromagnetic field and its spatial distribution. Thereafter, electromagnetic energy absorption which results in temperature increases within the human head and other interactions can be considered.

3.1. Physical model

In this study, a patch antenna of a mobile phone located at the left side of a human head with various gap distances is considered as near field radiation source for human head models. Fig. 2(a) shows the three-dimensional realistic human head model with the patch antenna used in this study at various gap distances between the patch antenna and the human head. This model comprises 4 types of tissue which are skin, fat, skull, and brain. These tissues have different dielectric and thermal properties. Fig. 2(b) gives the head dimensions used in this study, which are directly taken from statistical body-size data [16]. The dielectric properties and thermal properties of tissues are given in Tables 1 and 2, respectively.

3.2. Equations for electromagnetic wave propagation analysis

Mathematical models are developed to predict the electric field and SAR with relation to temperature gradient within the human head. To simplify the problem, the following assumptions are made:

Table 1
Dielectric properties of tissues [21,22].

Type of tissue	900 MHz		1800 MHz	
	ε_r	σ (S/m)	ε_r	σ (S/m)
Skin	41.41	0.87	32.5	0.52
Fat	11.33	0.11	5.35	0.078
Bone	20.79	0.34	8.0	0.16
Brain	45.805	0.765	53.0	1.7

Table 2
Thermal properties of tissues [13,23].

Tissue	ρ (kg/m^3)	k (W/m °C)	C_p (J/kg °C)	Q_{met} (W/m^3)	ω_b (1/s)
Skin	1125	0.42	3600	1620	0.02
Fat	916	0.25	3000	300	4.58E−04
Bone	1990	0.37	3100	610	4.36E−04
Brain	1038	0.535	3650	7100	8.83E−03

1. Electromagnetic wave propagation is modeled in three dimensions.
2. The human head in which electromagnetic waves and human head interaction proceeds in the open region.
3. The free space is truncated by scattering boundary condition.
4. The model assumes that dielectric properties of each tissue are constant.
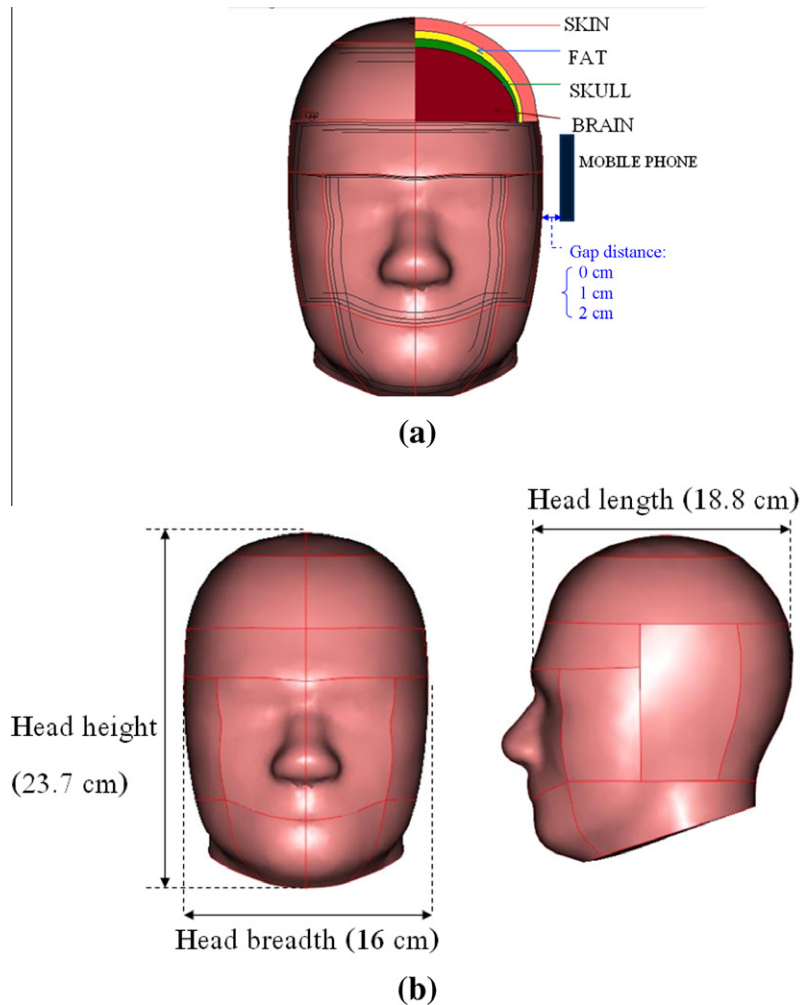

(a)

(b)

Fig. 2. Human head model, (a) cross section human head model with mobile phone, (b) dimensions of human head model.

The electromagnetic wave propagation in human head is calculated using Maxwell's equations [13,17], which mathematically describe the interdependence of the electromagnetic waves. The general form of Maxwell's equations is simplified to demonstrate the electromagnetic field penetrated in human head as the following equations:

$$\nabla \times \frac{1}{\mu_r} \nabla \times E - k_0^2 \varepsilon_r E = 0, \qquad (1)$$

where E is electric field intensity (V/m), μ_r is relative magnetic permeability, ε_r is relative dielectric constant, k_0 is the free space wave number (m^{-1}).

3.2.1. Boundary condition for wave propagation analysis

Electromagnetic energy is emitted by the patch antenna and strikes the human head with a particular radiated power. The lumped port, where it used to define a voltage drop across two patches, is placed between the two patches at the bottom of the patch antenna in order to generate an electromagnetic field. Therefore, the boundary conditions for solving electromagnetic wave propagation, as shown in Fig. 3, are described as follows:

At the bottom of the patch antenna, an electromagnetic simulator employs lumped port boundary condition with specified radiated power,

$$Z_{in} = \frac{V_1}{I_1} = \frac{E_1 l_1}{I_1} \qquad (2)$$

where Z_{in} is the input impedance (Ω), V_1 is the voltage along the edges (V), I_1 is the electric current magnitude (A), E_1 is the electric field along the source edge (V/m), l_1 is the edge length (m).

The patch of the antenna acts approximately as a cavity which the perfect electric conductor on the inner and outer surfaces is assumed. Hence, the perfect-electric-conductor boundary condition along the patches on the antenna is considered,

$$n \times E = 0 \qquad (3)$$

Boundary conditions along the interfaces between different mediums, for example, between air and tissue or tissue and tissue, are considered as continuity boundary condition,

$$n \times (E_1 - E_2) = 0 \qquad (4)$$

The outer sides of the calculated domain, i.e., free space, are considered as scattering boundary condition [7],

$$n \times (\nabla \times E) - jkn \times (E \times n) = -n \times (E_0 \times jk(n-k)) \exp(-jk \cdot r) \qquad (5)$$

where k is the wave number (m^{-1}), σ is electric conductivity (S/m), n is normal vector, $j = \sqrt{-1}$, and E_0 is the incident plane wave (V/m).

3.3. Interaction of electromagnetic waves and human tissues

When electromagnetic waves propagate through the human tissues, the energy of electromagnetic waves is absorbed by the tissues. Interaction of electromagnetic fields with biological tissues can be defined in term of **specific absorption rate** (SAR). The specific absorption rate is defined as power dissipation rate normalized by material density [13,18,20]. The specific absorption rate is described by the following equation:

$$SAR = \frac{\sigma}{\rho} |E|^2 \qquad (6)$$

where σ is electric conductivity (S/m), and ρ is the tissue density (kg/m^3).

3.4. Equations for heat transfer analysis

To solve the thermal problem, the temperature distribution in the human head has been evaluated by the bioheat equation which coupled to Maxwell's equations. The temperature distribution is corresponded to the specific absorption rate (SAR). This is because the specific absorption rate within the human head distributes owing to energy absorption. Thereafter, the absorbed energy is converted to thermal energy, which increases the tissue temperature.

Heat transfer analysis of the human head is modeled in three dimensions. To simplify the problem, the following assumptions are made:

1. Human tissues are bio-material with constant thermal properties.
2. There is no phase change of substance within the tissues.
3. There is no energy exchange throughout the boundary of human head model.
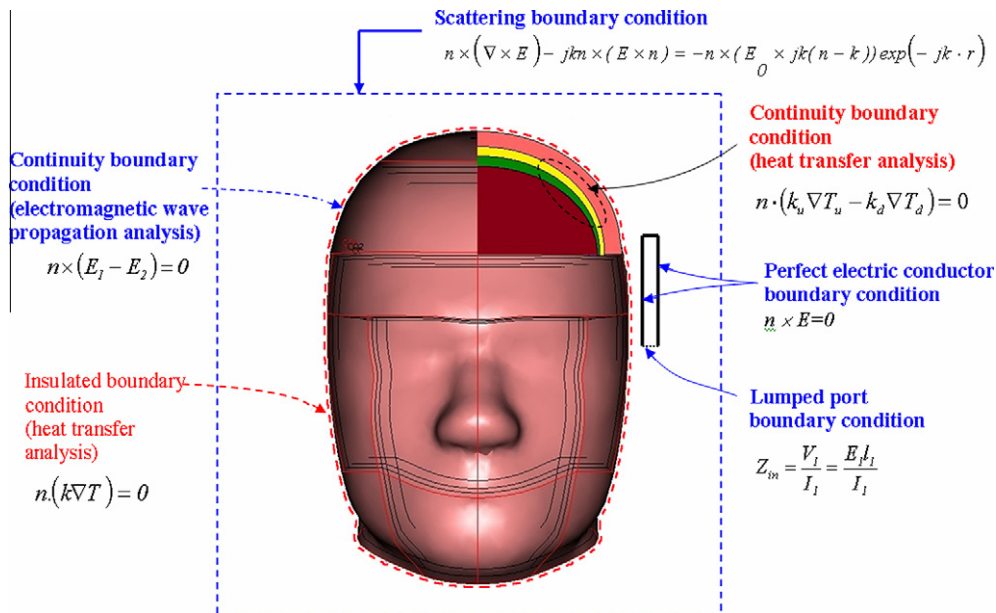4. There is no chemical reaction within the tissues.

Fig. 3. Boundary condition for analysis of electromagnetic wave propagation and heat transfer.

The temperature distribution within the human model is obtained by solving the Pennes' bio-heat equation [5,19] The transient bioheat equation effectively describes how heat transfer occurs within the human head, and the equation can be written as

$$\rho C \frac{\partial T}{\partial t} = \nabla \cdot (k \nabla T) + \rho_b C_b \omega_b (T_b - T) + Q_{met} + Q_{ext} \qquad (7)$$

where ρ is the tissue density (kg/m^3), C is the heat capacity of tissue (J/kg K), k is thermal conductivity of tissue (W/m K), T is the tissue temperature (°C), T_b is the temperature of blood (°C), ρ_b is the density of blood (kg/m^3), C_b is the specific heat capacity of blood (J/kg K), ω_b is the blood perfusion rate (1/s), Q_{met} is the metabolism heat source (W/m^3) and Q_{ext} is the external heat source term (electromagnetic heat-source density) (W/m^3).

In the analysis, heat conduction between tissue and blood flow is approximated by the blood perfusion term [5,13], $\rho_b C_b \omega_b (T_b - T)$.

The external heat source term is equal to the resistive heat generated by electromagnetic field (electromagnetic power absorbed), which defined as [13]

$$Q_{ext} = \frac{1}{2} \sigma_{tissue} |\bar{E}|^2 = \frac{\rho}{2} \cdot SAR \qquad (8)$$

where $\sigma_{tissue} = 2\pi f \varepsilon_r' \varepsilon_0$.

3.4.1. Boundary condition for heat transfer analysis

The heat transfer analysis is considered only in the human head, which does not include parts of the surrounding space. As shown in Fig. 3, the outer surface of human head corresponded to assumption (3) are considered as thermally insulated boundary condition,

$$n \cdot (k \nabla T) = 0 \qquad (9)$$

It is assumed that no contact resistant occurs between the internal organs of the human head. Therefore, the internal boundaries are assumed to be a continuity boundary condition,

$$n \cdot (k_u \nabla T_u - k_d \nabla T_d) = 0. \qquad (10)$$

3.5. Calculation procedure

In this study, the finite element method is used to analyze the transient problems. The computational scheme is to assemble finite element model and compute a local heat generation term by performing an electromagnetic calculation using tissue properties. In order to obtain a good approximation, a fine mesh is specified in the sensitive areas. This study provides a variable mesh method for solving the problem as shown in Fig. 4. The model of bioheat equation and Maxwell's equation are then solved. All computational processes are implemented using COMSOL^{TM} Multiphysics, to demonstrate the phenomenon that occurs within the human head exposed to electromagnetic field. The system of governing equations is solved with the unsymmetric multifrontal method. The electromagnetic power absorption at each point is computed and used to solve the time-dependent temperature distribution. All steps are repeated, until the required exposure time is reached. The calculation using time step for thermal model of 0.1 s and time step for electromagnetic field model of 10^{-11} s. The convergence criterion is specified at 10^{-6} and the maximum number of iterations is set to 1000 to assure that the transient solution is accurate. The 3D model is discretized using hexagonal elements and the Lagrange quadratic is used to approximate temperature and SAR variation across each element. Convergence test of the frequency of 900 MHz are carried out to identify the suitable number of elements required. The convergence curve resulting from the convergence test is shown in Fig. 5. This convergence test leads to the grid with approximately 200,000 elements. It is reasonable to assume
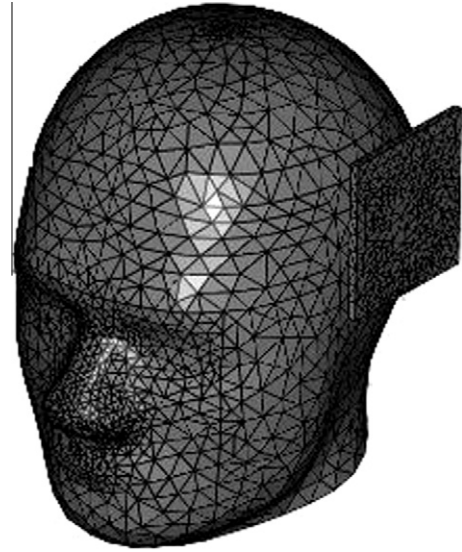

Fig. 4. A tree-dimensional finite element mesh of human head model.

that, at this element number, the accuracy of the simulation results is independent from the number of elements and therefore save computation memory and time. Higher numbers of elements are not tested due to lack of computational memory and performance.

4. Results and discussion

In this study, the mathematical model combining bioheat equation and Maxwell's equation for all cases are used for the analysis. For the simulation, the dielectric properties and thermal properties are directly taken from Tables 1 and 2, respectively. Since most GSM networks use frequencies in the 900 MHz and 1800 MHz spectrum, therefore, in this analysis, the effects of operating frequencies (900 MHz and 1800 MHz) and gap distances between the mobile phone and the human head (0 cm, 1.0 cm and 2.0 cm) on distributions of specific absorption rate and temperature profile within the human head are systematically investigated.

4.1. Verification of the model

It must be noted in advance that it is very difficult to make direct comparison of the model in this study and the experimental results because it is not possible to direct measure the temperature increase in the brain, especially in the case where the heating effect from mobile phone radiation is taken into account. Due to the geometry of the human head used to validate the numerical model is sparse. In order to verify the accuracy of the present numerical model, the modified case of the simulated results is then validated against the numerical results with the same geometric model obtained by Nishizawa and Hashimoto [20]. The SAR distribution in horizontal cross section of three layer human tissues as shown in Fig. 6 is used in the validation case. In the validation case, the leakage power density exposed to the electromagnetic frequency of 1300 MHz is 1 mW/cm^2. The results of the selected test case are illustrated in Fig. 7 for SAR distribution in the human tissues. Table 3 clearly shows a good agreement of the maximum value of the SAR of tissue between the present solution and that of Nishizawa with the maximum error of 3.88%. This favorable comparison lends confidence in the accuracy of the present numerical model. It is important to note that there may be some errors occurring in the simulations which are generated by the input dielectric properties and the numerical scheme.
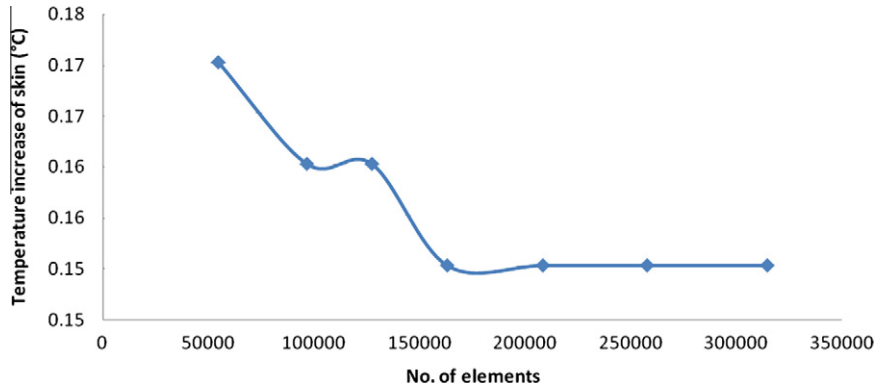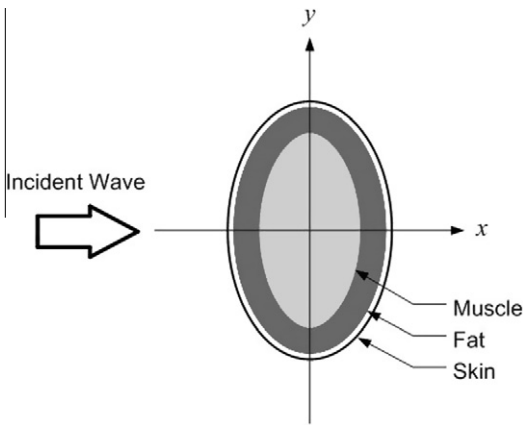
Fig. 5. Grid convergence curve of the 3D model.

Fig. 6. Geometry of the validation model obtained from the paper [20].

4.2. Electric field distribution

In order to study the effects of the operating frequency, a human head is exposed to the radiated power of 1 W at the frequencies of 900 MHz and 1800 MHz with the gap distance fixed to 1 cm for 30 min. Fig. 8 shows the simulation of electric field distribution within the human head exposed to mobile phone radiation along the extrusion line (Fig. 13) at the both frequencies. It can be seen that the higher values of electric field in both cases occur in the area
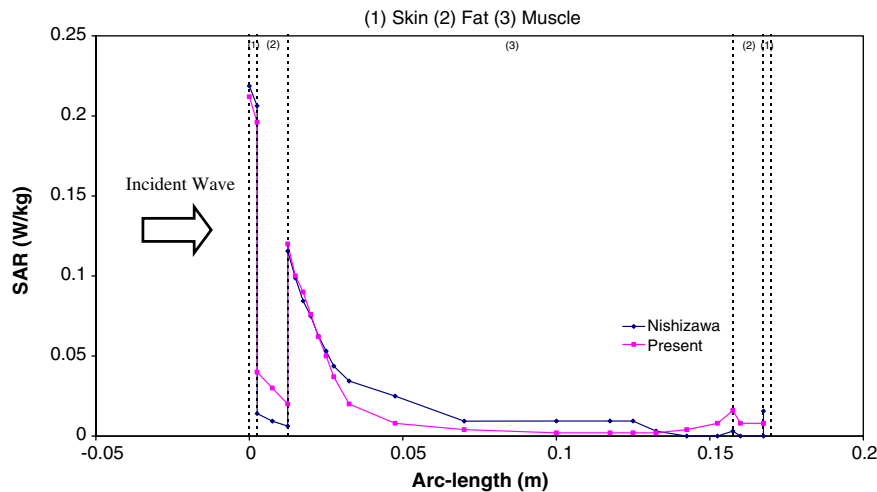
Table 3
Comparison of the results obtained in the present study with those of Nishizawa and Hashimoto [20].

	Present work	Published work [20]	% Difference
SAR_{max} in skin	0.212	0.220	3.63
SAR_{max} in fat	0.198	0.206	3.88
SAR_{max} in muscle	0.116	0.120	3.33

of outer parts of the head, especially in skin, and fat. By comparison, the maximum electric field intensity in outer parts of the human head at the frequency of 1800 MHz displays a higher value than that of 900 MHz. The maximum electric field intensities are 48.11 V/m at the frequency of 900 MHz and 135.25 V/m at the frequency of 1800 MHz. It is found that a large part of electromagnetic wave at 900 MHz can penetrate further into the human head. This electric field leads to deeper electromagnetic energy absorbed in the organs of human head in comparison to the frequency of 1800 MHz. With the lower frequency of 900 MHz, a large part of electromagnetic wave is able to penetrate into the human head due to its long wavelength has a stronger influence than the higher value of its dielectric properties (shown in Table 1) on the penetration of an electromagnetic field, which corresponds to a larger penetration depth. It is found that at the frequency of 1800 MHz, the electric field diminishes within small distances, which results in a low specific absorption rate in organs deep inside the human head. This phenomenon explains why the electric field and therefore the

Fig. 7. Comparison of the calculated SAR distribution to the SAR distribution obtained by Nishizawa and Hashimoto [20].
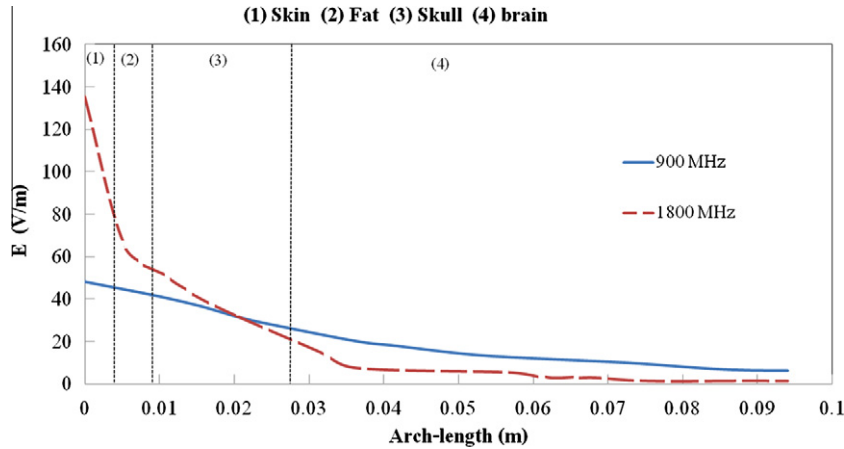
Fig. 8. Electric field distribution (V/m) in human head exposed to the radiated power of 1 W at the frequencies of 900 MHz and 1800 MHz, with 1 cm gap distance.

specific absorption rate are greatest at the skin and decay sharply along the propagation direction for a short wavelength.

4.3. SAR distribution

Fig. 9 shows the SAR distribution evaluated on the horizontal cross section of the human head. It is evident from the results that the dielectric properties as shown in Table 1 can become significant on SAR distribution in human tissues when electromagnetic energy is exposed in these tissues. The magnitude of dielectric properties in each tissue will directly affect the amount of SAR within the human head. The SAR pattern at the frequency of 900 MHz shows greater electromagnetic power absorption in the deep part of the human head, with less surface heating, compared to those of 1800 MHz. For both frequencies, the highest SAR values are obtained in the region of the skin near the antenna. The frequency of 900 MHz displays SAR of 0.823 W/kg and for the frequency of 1800 MHz displays SAR of 1.187 W/kg. It is found that the SAR distribution pattern in the human head is depended on the effect of the frequency and the dielectric properties of human tissues. With penetration into the head, the SAR values decrease rapidly along the

distance. However, it can be observed a deeper penetration of the electromagnetic energy within the human head in the 900 MHz frequency; this corresponds to an electric field distribution (Fig. 8). The SAR distributions in the human head are found to be correlated with the electric field distributions (Figs. 8). Comparing to ICNIRP limit of SAR value (2 W/kg), the resulting SAR from this study are not exceeded limit value in all cases. The SAR distribution in each tissue are presented in detail in Section 4.5.

4.4. Temperature distribution

In order to study the heat transfer within the human head, the coupled transport phenomenon of electromagnetic wave propagation and unsteady bioheat transfer are then investigated. Due to these coupled phenomena, the electromagnetic energy (Fig. 8) is absorbed by the tissues (Fig. 9) and this energy is then converted into heat. Fig. 10 shows the temperature distribution in the horizontal cross section human head exposed to the radiated power of 1 W with 1 cm gap distance for 30 min at the frequencies of 900 MHz (Fig. 10(a)) and 1800 MHz (Fig. 10(b)). Fig. 10(c) shows the steady state temperature distribution in the human head in
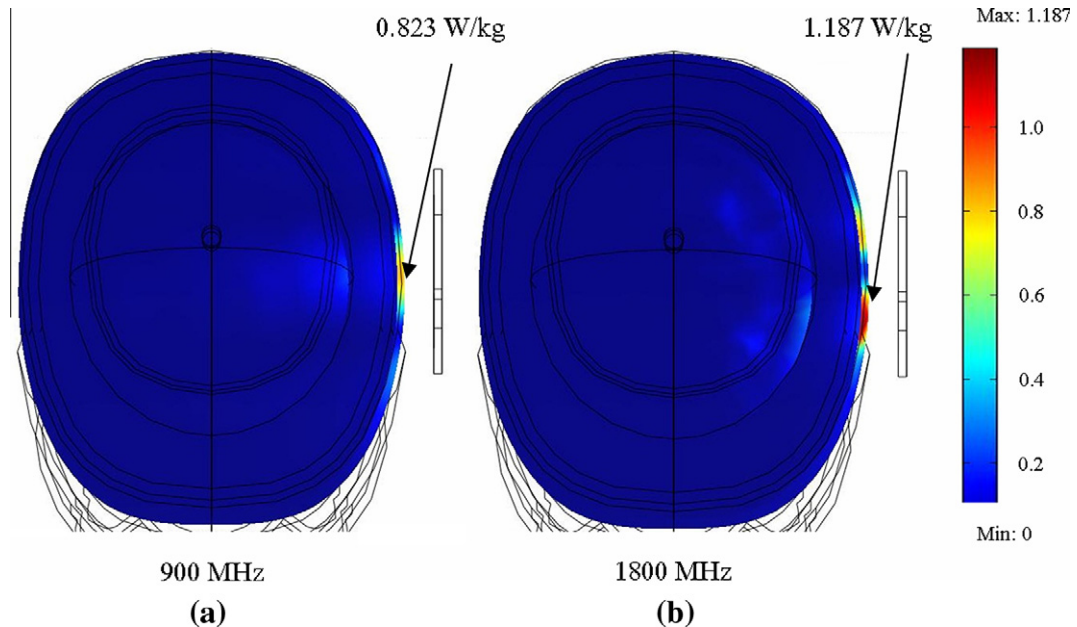

Fig. 9. SAR distribution (W/kg) in human head exposed to the radiated power of 1 W at the frequencies of (a) 900 MHz and (b) 1800 MHz, with 1 cm gap distance.
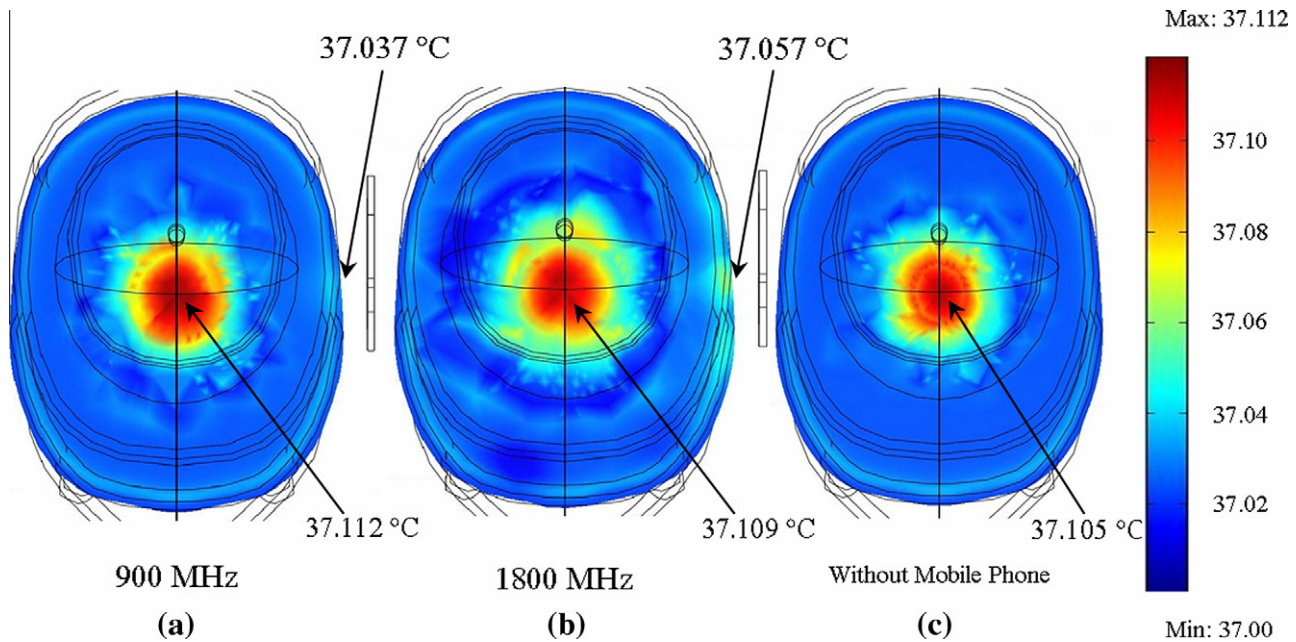
Fig. 10. The temperature distribution in human head exposed to the radiated power of 1 W with 1 cm gap distance for 30 min. (a) At the frequency of 900 MHz. (b) At the frequency of 1800 MHz. (c) The temperature distribution in human head without mobile phone used.

case of without the mobile phone. For the human head exposed to the mobile phone radiation, the temperature within the human head (Fig. 10(a) and (b)) is increased corresponding to the specific absorption rate (Fig. 9). This is because the electric field within the human head attenuates owing to the energy absorbed and thereafter the absorbed energy is converted to thermal energy, which increases the human head temperature. Nevertheless, in regions of weak electric field intensity, metabolic heat generation as well as blood perfusion becomes the dominant mechanism for heat transfer. The maximum temperature increases are small in all cases. It is found that at the different frequencies, the temperature distribution patterns are quite different. For both frequencies, the hot spot zone is strongly displayed at the skin and brain tissue. In the skin region, the case of 1800 MHz has higher temperature (37.057 °C) than that of the 900 MHz (37.037 °C). While in the brain region, the 900 MHz has higher temperature (37.112 °C) than that of the 1800 MHz (37.109 °C). The temperature increases in the human head are found to be correlated with the electric field and SAR (Figs. 8 and 9). There are much lower than the thermal damage temperature of 3.5 °C [3]. The brain is a tissue with high metabolic heat generation, and consequently resulting in a higher temperature of brain tissue than the other tissues with lower metabolic heat generation. While the temperature in skin region is lower than that of brain region even if it has higher SAR value than other tissues. This is due to the higher blood perfusion of the skin tissue plays an important role to keep a low temperature of the tissue. It can be seen that, the maximum temperature increase observed in each frequency is not much different; however the observed temperature distribution pattern in each frequency is significantly different and is dominated by the dielectric properties and thermal properties of the tissues. The temperature distribution in each tissue will be presented in detail again in Section 4.5.

4.5. Comparison of SAR distribution and temperature distribution in human tissues

In order to study the comparison of SAR distribution and temperature distribution within the human head, the SAR and temper-

ature distribution along an extrusion line are then investigated. Figs. 11 and 12, respectively, show the slice plot of SAR distribution and the temperature distribution of human head exposed to the radiated power of 1 W at the frequency of 900 MHz for 30 min with no gap distance and with 1 cm gap distance. The slice plot in Figs. 9 and 10 showing the sensitive area of SAR and temperature distribution within the human head that gives important information to select the appropriate extrusion line as shown in Fig. 13.

In Fig. 13, consider the relation of SAR and temperature distribution at the extrusion line, the temperature increases of human tissues are induced by local dissipation of SAR. Fig. 14 shows the SAR distribution versus arc-length of human head exposed to the radiated power of 1 W with 1 cm gap distance for 30 min. With penetration into the head, the SAR values decrease rapidly along the distance. However, it can be observed a deeper penetration of the electromagnetic energy within the human head in the 900 MHz frequency; this corresponds to an electric field distribution (Fig. 8). The graph shows the higher SAR values of the 1800 MHz frequency at the skin, fat and brain periphery. While in the skull and middle brain region, the SAR value of 1800 MHz frequency is lower than that of 900 MHz. This is because at the frequency of 1800 MHz, skull has a much lower electrical conductivity than that of 900 MHz and the electric field intensity at 1800 MHz is decreasing rapidly. The SAR distribution in Fig. 14 is correlated with the temperature distribution in Fig. 15. However, the maximum temperature of the 900 MHz frequency is found to be higher than that of 1800 MHz frequency, especially in the middle brain region. This is due to a deeper penetration of the electric field and SAR pattern into the human head of the 900 MHz frequency. Upon the thermal parameters shown in Table 2, the thermal conduction effect causes the 1800 MHz frequency has a higher temperature in bone even if it has lower SAR value than that of 900 MHz. This behavior is due to the fact that for the different frequency radiation at same radiated power, the temperature distribution is not the same.

Fig. 16 shows the localized maximum SAR values of human head exposed to the radiated power of 1 W with 1 cm gap distance
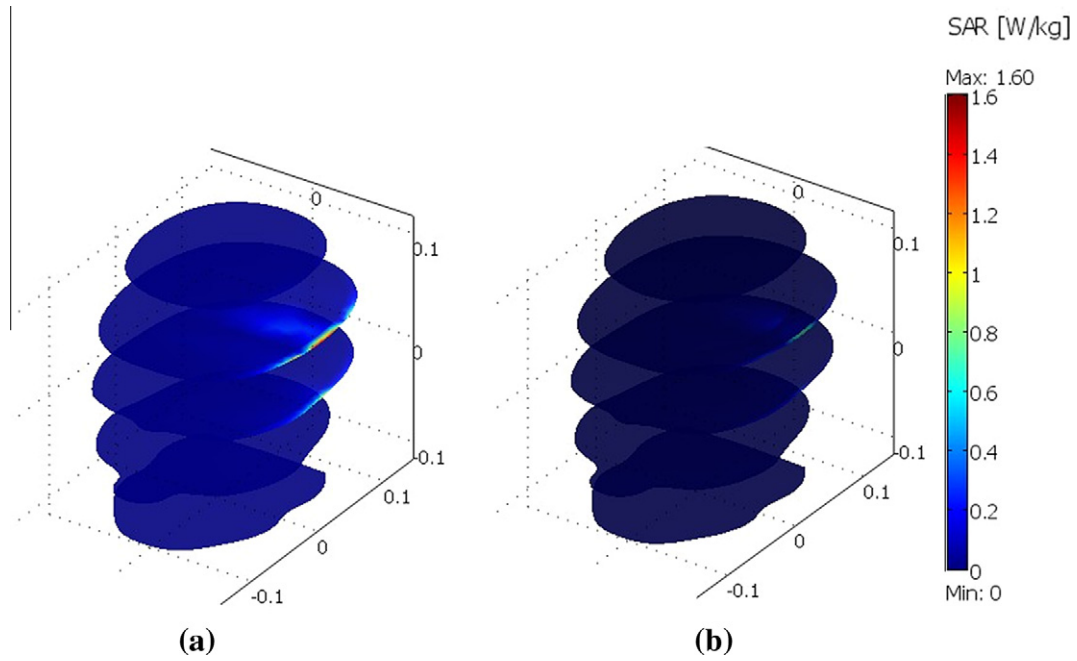
Fig. 11. The slice plot of SAR distribution in human head exposed to the radiated power of 1 W at the frequency of 900 MHz (a) with no gap distance (b) with 1 cm gap distance.
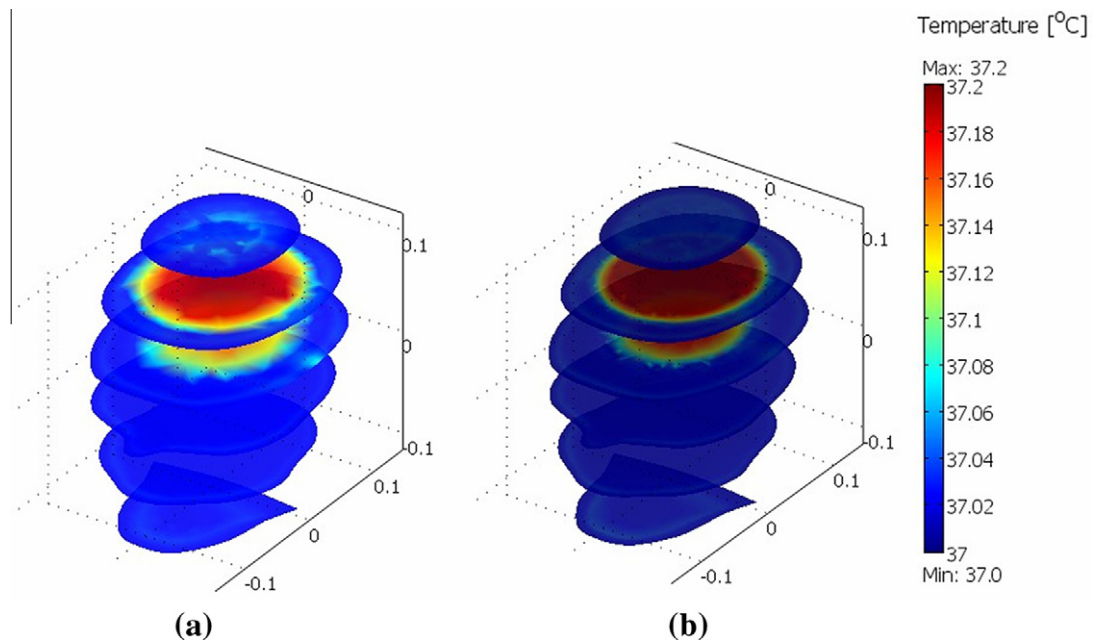

Fig. 12. The slice plot of temperature distribution exposed to the radiated power of 1 W at the frequency of 900 MHz (a) with no gap distance (b) with 1 cm gap distance.

for 30 min for the frequencies of 900 MHz and 1800 MHz. For the value of localized SAR for each tissue layer, it is found that SAR distribution is corresponded to electric field distribution as well as the dielectric properties of tissues. For both frequencies, the highest SAR values are shown for skin tissue and brain tissue, respectively. Furthermore, most of the localized SAR for each tissue of the 1800 MHz frequency is higher than that of the 900 MHz frequency except bone tissue. This is because at the frequency of 1800 MHz, bone has a much lower electrical conductivity than that of 900 MHz, while the electric field intensities in bone are insignificant difference between these two frequencies.

Fig. 17 shows the localized maximum temperature increases of human head exposed to the radiated power of 1 W with 1 cm gap distance for 30 min for the frequencies of 900 MHz and 1800 MHz. The highest temperature increase in both frequencies occurs in skin, fat, bone, and brain, respectively. It is observed that the second highest temperature increase in both frequencies appears in the fat tissue, not in brain like the SAR values as shown in Fig. 16. This is because fat tissue has lower blood perfusion rate (4.58×10^{-4} 1/s) than the brain (8.83×10^{-3} 1/s) which causes the heat transfer due to blood perfusion is less effective in fat. At the same time, there is also the contribution of heat conduction

from the skin tissue, which displays a strong influence on the fat and bone temperature.

In addition, it is found that the temperature distributions are not directly related to the SAR distribution. Nevertheless, these are also related to the parameters such as; thermal conductivity, dielectric properties, blood perfusion rate and etc. It is therefore important to use a strongly coupled model of thermal and electromagnetic wave propagation model to asses the health effects of exposure to electromagnetic wave radiated by the mobile phone.
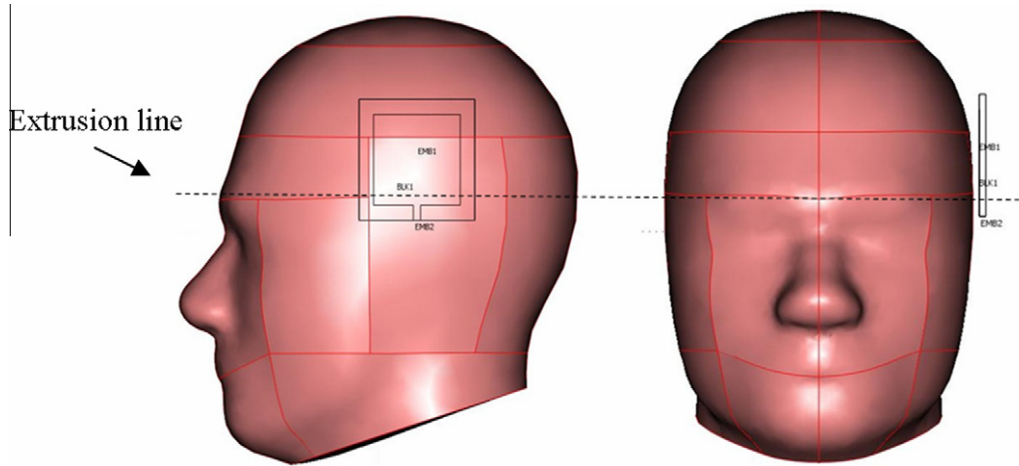
Fig. 13. The extrusion line in the human head where the SAR and temperature distribution are considered.
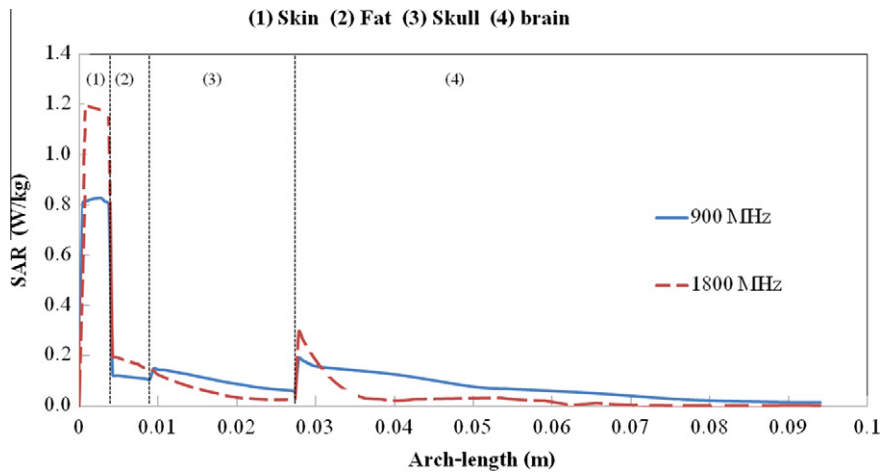
Fig. 14. SAR distribution versus arc-length of human head exposed to the radiated power of 1 W with 1 cm gap distance for 30 min.
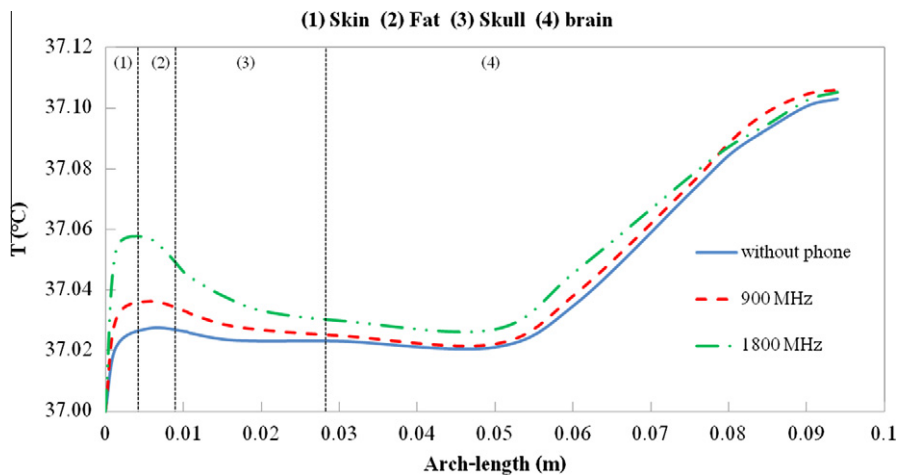

Fig. 15. Temperature distribution versus arc-length of human head exposed to the radiated power of 1 W with 1 cm gap distance for 30 min.
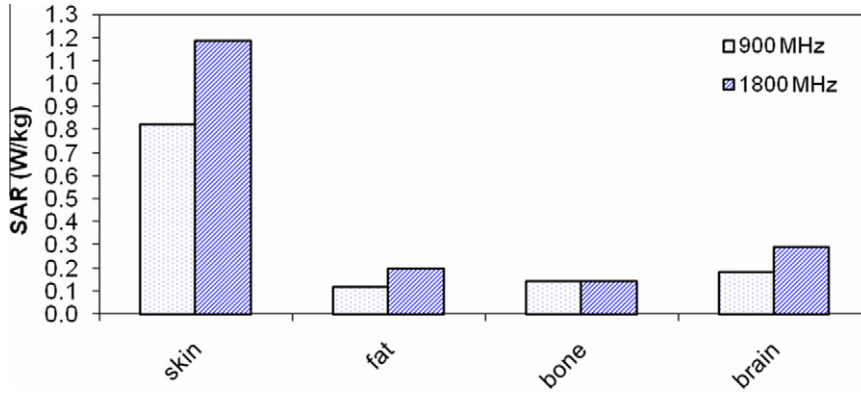
Fig. 16. Comparison of the maximum SAR in human tissues of human head exposed to the radiated power of 1 W at the frequencies of 900 MHz and 1800 MHz, with 1 cm gap distance for 30 min.
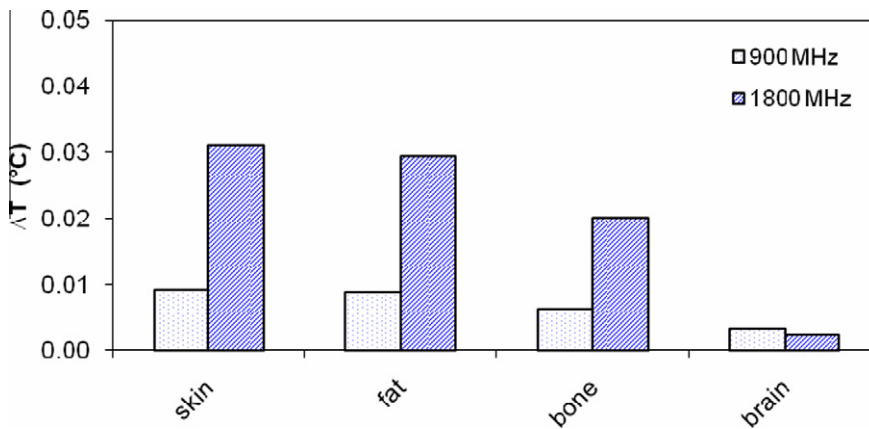

Fig. 17. Comparison of the temperature increases in human tissues of human head exposed to the radiated power of 1 W with 1 cm gap distance for 30 min.

4.6. Effect of gap distance between the mobile phone and the human head

The effect of gap distance between the mobile phone and the human head has also investigated. Fig. 18 shows the comparison of the SAR distribution within the human head at various gap distances with the radiated powers of 1.0 W at the frequency of 900 MHz for 30 min, along the extrusion line (Fig. 13). As the gap distance decreases, the maximum SAR value in the skin tissue is increased. The maximum SAR values are 0.4, 0.8 and 1.6 W/kg for the

gap distances of 2.0, 1.0 and 0 cm, respectively. Fig. 19 shows the temperature distribution within the human head along the extrusion line corresponding to gap distances of 0 cm, 1.0 cm and 2.0 cm. As the gap distance decreases, the maximum temperature is increased as well, but the gap distance contributes low influence to the midbrain region because the high blood perfusion of brain tissue plays an important role to keep a low temperature of the midbrain region. It is found that gap distance between the mobile phone and the human head significantly influences the SAR and temperature distribution. This is due to a smaller gap distance
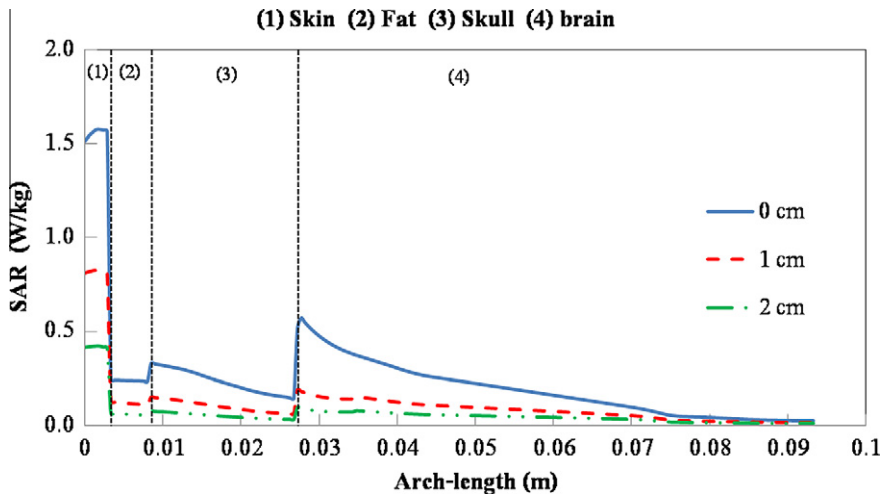

Fig. 18. SAR distribution versus arc-length of human head exposed to the radiated power of 1 W at the frequency of 900 MHz at various gap distances for 30 min.

Fig. 19. Temperature distribution versus arc-length of human head exposed to the radiated power of 1 W at the frequency of 900 MHz at various gap distances for 30 min.

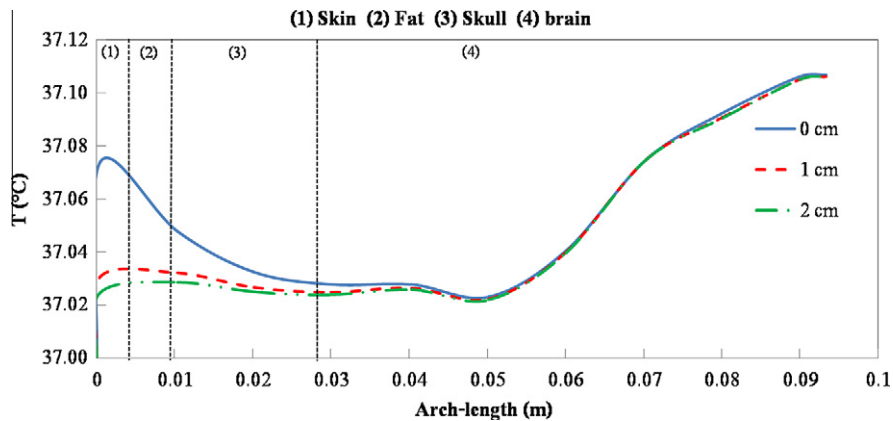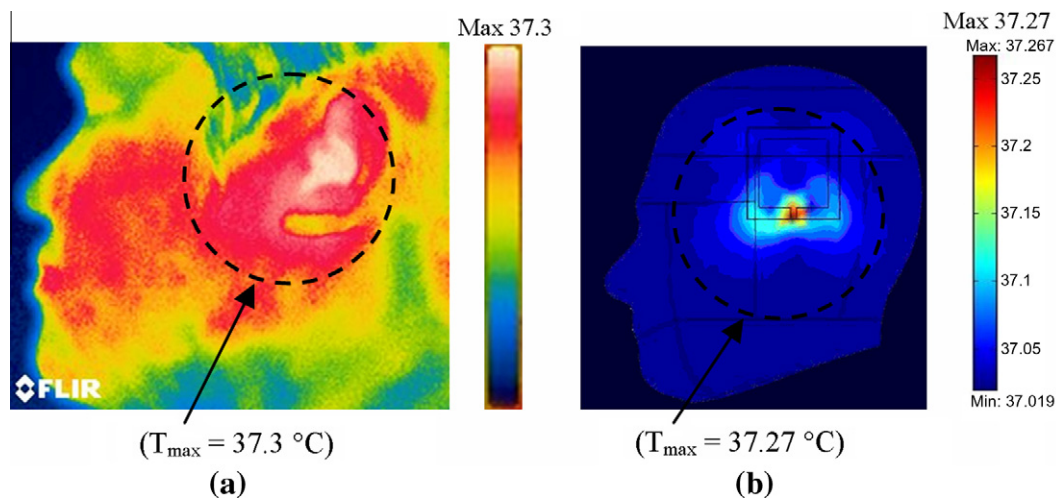

Fig. 20. Comparison between experimental result (a) and simulated result (b) of surface temperature distribution (°C) of human head after exposed to the 1800 MHz mobile phone radiation at the radiated power of 1 W with no gap distance for 30 min.

leads to higher electric field intensities, SAR, and heat generation inside the human head, thereby increasing the temperature within the human head.

The experiment was set up in an indoor nonairconditioned environment. The room temperature was approaching to the temperature of human body of 37 °C. A FLIR t200 infrared camera was used to measure the surface temperature of the human head. The parameters setting of the system were: emissivity = 0.98, subject distance = 30 cm, RH = 0.8. Fig. 20 shows the comparison between simulated result and experimental result (measured by infrared camera) of surface temperature distribution of human head exposed to the radiated power of 1 W with no gap distance for 30 min at the frequency of 1800 MHz. The results show the greatest temperature in the pinna region especially near the feed point of the antenna where the maximum electric field is occurred, while the other areas display the lower temperature. The maximum temperature found in the experimental result is 37.3 °C compared to 37.27 °C of the simulated result. It can be seen that the agreement between the two temperature distributions is good, particularly concerning the location of the hot region.

5. Conclusions

This study presents the numerical simulation of SAR and temperature distribution in the realistic human head model exposed to mobile phone radiation at the frequencies of 900 MHz and 1800 MHz with various gap distances between the mobile phone and the human head. The numerical simulations in this study show several important features of the energy absorption in the human head.

In all cases of exposure, the highest SAR in the human head occurred near the surface, directly beneath the feed point of the mobile phone antenna. Refer to the SAR limit recommended by the ICNIRP of 2 W/kg, the SAR values obtained from this study are well below ICNIRP limit for all cases.

In the human head, the location for the maximum temperature increase is not necessarily the same as for the maximum SAR due to various mechanisms of electromagnetic propagation and heat transfer. In view of the fact that the temperature distributions do not always correlate well with the SAR distributions. The maximum temperature increase in skin of 1800 MHz frequency is higher than that of 900 MHz frequency. While the maximum temperature increases in brain of 1800 MHz frequency is lower than that of 900 MHz frequency. In all cases of exposure, the temperature increases calculated in this study are lower than the thresholds for the induction of thermal damage in all the considered situations.

A smaller gap distance between the mobile phone and the human head leads to higher electric field intensities, SAR, and heat generation inside the human head, thereby increasing the temperature

within the human head. Moreover, it is found that the temperature distributions in human head induced by mobile phone radiation are not directly related to the SAR distribution due to the effect of dielectric properties, thermal properties, blood perfusion, and penetration depth of the electromagnetic power.

Therefore, health effect assessment of mobile phone radiation requires the utilization of the numerical simulation of SAR model along with the thermal model. This will allow a better understanding of the realistic situation of the interaction between electromagnetic field from mobile phone radiation and the human tissues.

Acknowledgments

References

[1] A.C. Guyton, J.E. Hall, Medical Physiology, Saunders, Philadelphia, PA, 1996 (ch. 73).

[2] E.R. Adair, B.W. Adams, G.M. Akel, Minimal changes in hypothalamic temperature accompany microwave-induced alteration of thermoregulatory behavior, Bioelectromagnetics 5 (1984) 13–30.

[3] International Commission on Non-Ionizing Radiation Protection (ICNIRP), Guidelines for limiting exposure to time-varying electric, magnetic and electromagnetic fields (up to 300 GHz), Health Phys. 74, (1998) 494–522.

[4] IEEE, IEEE Standard for Safety Levels with Respect to Human Exposure to Radio Frequency Electromagnetic Fields, 3 kHz to 300 GHz, IEEE Standard C95 1-1999.

[5] H.H. Pennes, Analysis of tissue and arterial blood temperatures in the resting human forearm (reprint of 1948 article), J. Appl. Physiol. 85 (1998) 5–34.

[6] D. Yang, M. Converse, D. Mahvi, Expanding the bioheat equation to include tissue internal water evaporation during heating, IEEE Trans. Biomed. Eng. 54 (8) (2007) 1382–1388.

[7] J. Okajima, S. Maruyama, H. Takeda, Dimensionless solutions and general characteristics of bioheat transfer during thermal therapy, J. Therm. Biol. 34 (8) (2009) 377–384.

[8] K.J. Chua, S.K. Chou, On the study of the freeze-thaw thermal process of a biological system, Appl. Therm. Eng. 29 (17–18) (2009) 3696–3709.

[9] A. Nakayama, F. Kuwahara, A general bioheat transfer model based on the theory of porous media, Int. J. Heat Mass Transfer 51 (2008) 3190–3199.

[10] S. Mahjoob, K. Vafai, Analytical characterization of heat transfer through biological media incorporating hyperthermia treatment, Int. J. Heat Mass Transfer 52 (5–6) (2009) 1608–1618.

[11] A. Sakurai, S. Maruyama, K. Matsubara, The radiation element method coupled with the bioheat transfer equation applied to the analysis of the photothermal effect of tissues, Numer. Heat Transfer Part A 58 (2010) 625–640.

[12] O.P. Gandhi, G. Kang, Some present problems and a proposed experimental phantom for SAR compliance testing of cellular telephones at 835 MHz and 1900 MHz, Phys. Med. Biol. 47 (2002) 1501–1518.

[13] T. Wessapan, S. Srisawatdhisukul, P. Rattanadecho, Numerical analysis of specific absorption rate and heat transfer in the human body exposed to leakage electromagnetic field at 915 MHz and 2450 MHz, ASME J. Heat Transfer 133 (2011) 051101-1–051101-13.

[14] T. Wessapan, S. Srisawatdhisukul, P. Rattanadecho, The effects of dielectric shield on specific absorption rate and heat transfer in the human body exposed to leakage microwave energy, Int. Commun. Heat Mass Transfer 38 (2) (2011) 255–262.

[15] P. Keangin, P. Rattanadecho, T. Wessapan, An analysis of heat transfer in liver tissue during microwave ablation using single and 2 double slot antenna, Int. Commun. Heat Mass Transfer 38 (6) (2011) 757–766.

[16] J. Wang, O. Fujiwara, Comparison and evaluation of electromagnetic absorption characteristics in realistic human head models of adult and children for 900 MHz mobile telephones, IEEE Trans. Microw. Theor. Tech. 51 (2003) 966–971.

[17] R.J. Spiegel, A review of numerical models for predicting the energy deposition and resultant thermal response of humans exposed to electromagnetic fields, IEEE Trans. Microw. Theor. Tech. 32 (8) (1984) 730–746.

[18] H. Kanai, H. Marushima, N. Kimura, T. Iwaki, M. Saito, H. Maehashi, K. Shimizu, M. Muto, T. Masaki, K. Ohkawa, K. Yokoyama, M. Nakayama, T. Harada, H. Hano, Y. Hataba, T. Fukuda, M. Nakamura, N. Totsuka, S. Ishikawa, Y. Unemura, Y. Ishii, K. Yanaga, T. Matsuura, Extracorporeal bioartificial liver using the radial-flow bioreactor in treatment of fatal experimental hepatic encephalopathy, Artif. Organs 31 (2) (2007) 148–151.

[19] D. Yang, M.C. Converse, D.M. Mahvi, J.G. Webster, Expanding the bioheat equation to include tissue internal water evaporation during heating, IEEE Trans. Biomed. Eng. 54 (8) (2007) 1382–1388.

[20] S. Nishizawa, O. Hashimoto, Effectiveness analysis of lossy dielectric shields for a three-layered human model, IEEE Trans. Microw. Theor. Tech. 47 (3) (1999) 277–283.

[21] J. Wang, O. Fujiwara, S. Watanabe, Approximation of aging effect on dielectric tissue properties for SAR assessment of mobile telephones, IE EE Trans. Electromagnetic Compat. 48 (2) (2006) 408–413.

[22] S. Park, J. Jeong, Y. Lim, Temperature rise in the human head and brain for portable handset at 900 and 1800 MHz, in: Proceedings of the Fourth Microwave and Millimeter Wave Technology Conference, IEEE, Beijing, China, (2004) 966–969.

[23] A. Hirata, O. Fujiwara, T. Shiozawa, Correlation between peak spatial-average SAR and temperature increase due to antennas attached to human trunk, IEEE Trans. Biomed. Eng. 53 (8) (2006) 1658–1664.